Appendix C: Cross-Frame Design Example (Curved Bridge)

Introduction

This document follows the Steel Bridge Design Handbook (SBDH) Design Example 3: Three-Span Continuous Horizontally Curved Composite Steel I-Girder Bridge (Rivera and Chavel 2015). In that example, girder design and detailing is evaluated extensively. Based on the findings and results of NCHRP Project 12-113, the calculations presented herein expand on SBDH Design Example 3. In general, the calculations follow AASHTO *LRFD* 9th Edition Specifications (2020), or as modified based on the recommendations of NCHRP 12-113. The proposed recommendations are discussed and illustrated with sample calculations. For clarity, AASHTO *LRFD* article numbers are simply referred to as Article 4.6.3 (as an example) herein.

This document focuses on three major components of cross-frame design: (i) analysis techniques, (ii) combining force effects including stability bracing requirements, and (iii) estimating the capacity/resistance for all relevant limit states. Following this brief introductory section and an overview of pertinent AASHTO *LRFD* Articles, the calculation herein is organized by those three components. Relevant information such as cross-section views, if not included in this document, can be found in the original design example. For reference, a framing plan adapted from Rivera and Chanel (2015) is provided below.

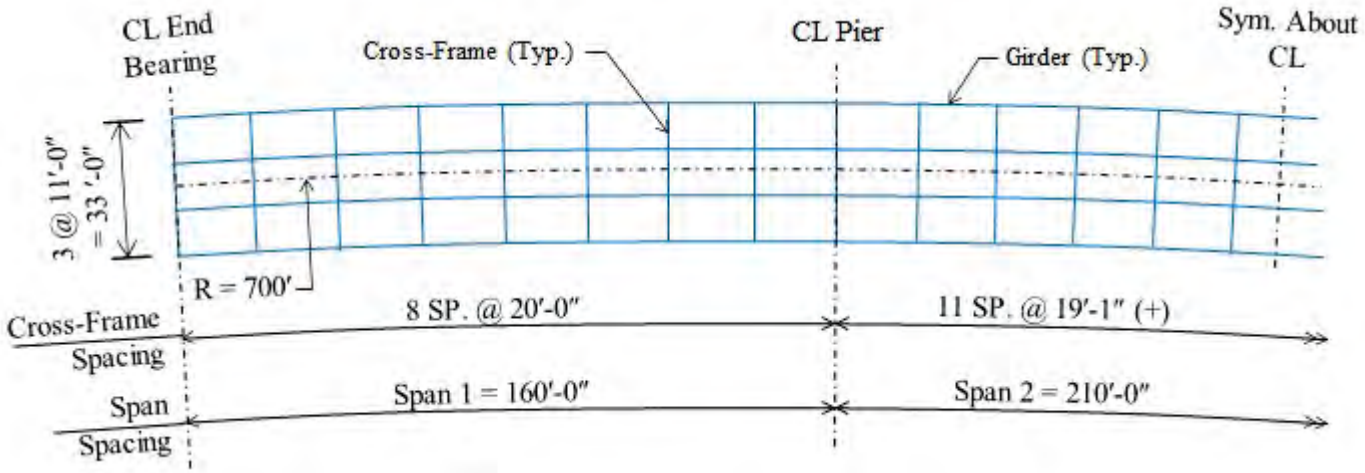

Figure 1: Sketch of superstructure faming plan of bridge; adapted from Rivera and Chavel (2015)

Parameters highlighted in yellow are user inputs (e.g., geometric properties, material properties, design constants). Parameters that are not highlighted have either been previously defined or are functions of other values input by the user. Results highlighted in red are key design loads or resistances, and final design checks are highlighted in orange.

AASHTO LRFD Overview

As outlined in Article 6.7.4, cross-frames shall be investigated for all stages of assumed construction procedures and the final condition. Cross-frames serve many purposes and resist a variety of loads throughout the life of a bridge. Those loading conditions, for which a designer should consider in design, include the following:

- Transfer of lateral wind loads from the bottom of the girder to the deck and from the deck to the bearings;
- Provide lateral support to the fascia girders between cross-frame locations to control torsional stresses and rotations due to loads applied to the overhangs, particularly during concrete deck placement;
- Control stability of the girder in the negative and positive moment region by restraining twist of the cross-section prior to curing of the concrete deck;
- Consideration of any flange lateral bending effects; and
- Distribution of vertical dead and live loads applied to the structure.

Also documented in Article 6.7.4, cross-frames shall be designed for all applicable limit states, if included in the structural model used to determine force effects. This is particularly true for horizontally curved bridges

that exceed one or more of the conditions specified in Article 4.6.1.2.4 for neglecting the effects of curvature. In these cases, the force effects in cross-frames (considered primary members) shall be computed, and all applicable limit states shall be considered in the design of the member and connections. For straight bridges, at a minimum, cross-frames shall be designed to transfer wind loads according to the provisions of Article 4.6.2.7 and shall meet all applicable slenderness requirements in Article 6.8.4 or Article 6.9.3. Although, as recommended from NCHRP 12-113, stability bracing should also be considered a minimum design requirement.

SBDH Example 3 represents a three-span, horizontally curved bridge with normal supports. Therefore, cross-frames are considered primary members and shall be comprehensively designed for all limit states. In the original SBDH Example 3 document, cross-frames and their connection plates were only designed for select load cases. In this calculation, a more thorough investigation of all pertinent design checks is made. For reference, the cross-frames are spaced at 20 feet on center typically and are placed in contiguous, radial lines oriented normal to the girders; this layout is in compliance with the guidelines provided in Article 6.7.4.2. Additionally, the cross-frame spacing satisfies the spacing limits established for curved systems in the same article, as was documented in Section 4.5 of the original design example.

To better understand the response of cross-frames during construction and in the final composite structure, this extended design calculation evaluates additional load conditions including: overhang construction, stability bracing during steel erection, dead loads, and wind loads (during construction and in the final composite system). In curved systems, centrifugal forces are typically considered; however, for purposes of cross-frame design, it is assumed that these lateral forces are resolved entirely by the concrete deck.

Wind loads and overhang construction loads are often determined by simple hand calculation methods. Stability bracing loads, for curved systems, can be determined from simplified methods or performing a large-displacement analysis provided that imperfections are considered (Helwig and Yura, 2015). For the sake of simplicity, simplified hand solutions are used in this calculation. For bridges with significant curvature, stability forces and the impact of initial imperfections tend to be less significant when compared to other load cases. This assertion is investigated in this calculation set.

In contrast, dead load (staged construction and final constructed state) and live load effects in curved systems can be obtained from refined computer analyses or estimated with simplified techniques. For improved reliability and to maintain consistency with the original design example, 3D analysis methods are the focus herein. With that in mind, first-order analyses, which have been shown by Stith et al. (2010) to produce accurate results for laterally stiff girders (i.e., b_f/d exceeding 1/4), were conducted. A more detailed discussion on these load cases is provided in subsequent sections.

Analysis Techniques

As noted previously, refined computer analysis is often used to determine dead and live load force effects in curved bridge superstructures, especially for primary elements such as cross-frames. Load-induced cross-frame forces can be substantial in curved and/or skewed systems, as demonstrated by the results of NCHRP 12-113. In fact, geometric skew and curvature limits were established and proposed for AASHTO *LRFD* implementation for when live load forces need to be considered for cross-frame design. Because the connectivity index of this bridge (1.34; as determined by the equation established in Article 4.6.3.3.2) exceeds I_c = 1.0, a refined analysis is recommended. As such, refined analysis methods, including approximate methods (V-load), 2D analysis, and 3D analysis are permitted for determining live load force effects for both the strength and fatigue limit states per AASHTO 3.6.1.

In terms of selecting the appropriate analysis, the results of NCHRP 12-113 demonstrated that 3D models consistently produce more reliable cross-frame results than comparable 2D models given that the depth of the superstructure is explicitly considered and complex load paths associated with curved systems are more accurately represented. Although 2D analysis approaches (e.g., grid/grillage, eccentric plate and beam) are permitted, a 3D approach was used to best demonstrate the recommended analysis and design practices for

cross-frames, similar to the original design example.

The 3D model developed qualifies as a refined analysis technique, as defined in Articles 4.4 and 4.6.3. A relatively common commercial software package was utilized to develop the structural model. The geometry was developed in accordance with the geometric parameters outlined in the original Design Example 3 document (Rivera and Chavel 2015), and the model is representative of what most design engineers would develop for a comparable bridge structure. A staged construction analysis, as well as the final constructed condition, are evaluated. First-order analyses were conducted for all stages of construction based on the discussion above; second-order effects are assumed negligible given the girder proportions.

The model is comprised of shell elements for deck and girder elements and pin-ended truss elements for cross-frame members. In the original design example, the analysis was performed assuming a gross cross-sectional area of 5 sq. inches for cross-frames, but the resistance design assumed 11.5 sq. inches. To maintain consistency, L8x8x3/4 single angles (11.4 sq. inches) are used in the analysis model and design here. Composite action is simulated by vertically offsetting and restraining relative movement between nodes in the top flange and deck shells. Bearings are modeled as linear spring elements, whose lateral stiffness is consistent with common bearings documented in Section 14 of AASHTO *LRFD*.

Another focal point of NCHRP Project 12-113 was the development of appropriate modification factors for eccentrically-loaded single-angle members, from which cross-frames are commonly constructed. Cross-frame systems, which consist of connection plates, gusset plates, and angle members connected via welds and/or bolts, are typically simplified in structural analysis models as pin-ended truss elements. The assumed stiffness, with no modification factor, is generally greater than the true stiffness. It is imperative that the engineer represent the actual stiffness of the cross-frame in the analysis model; overestimating the cross-frame stiffness is conservative from a fatigue perspective but unconservative from a stability bracing perspective.

AASHTO *LRFD* 9th Edition recommends applying a uniform modification factor of 0.65 (C4.6.3.3.4) based on the research conducted by Battistini et al. (2016) for stability-related applications. From the work conducted as part of NCHRP 12-113, it is recommended that an R-factor of 0.75 is more appropriate for the response of cross-frame systems in composite structures subjected to traffic loads. This modification factor can either be assigned to the cross-sectional area of the truss element or the modulus of elasticity of the material properties. Note that R = 0.65 is still appropriate for the construction condition.

It was also shown from the results of NCHRP 12-113 that modeling the cross-frame members as eccentric beam elements produces accurate force predictions when compared to a model comprised of shell-element cross-frames. This method is an acceptable alternative to the R-factor approach but is not demonstrated in this example. For reference, a screenshot of the 3D model during its final constructed stage is presented.

In-service modification factor: $R_{ser} := 0.75$

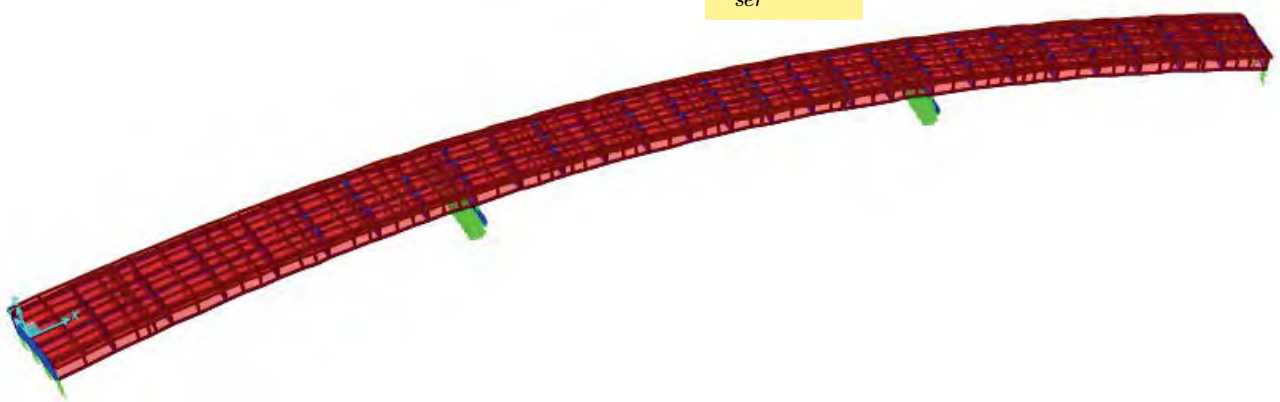

Figure 2: Screenshot of the 3D analysis model

To estimate the live-load force effects in the cross-frame members for both strength and fatigue limit states, an influence-surface analysis was conducted. Influence-surface analyses facilitate the handling of moving loads in design; many commercial software packages have built-in capability to perform this special analysis. If not inherently built into the program, the engineer is still tasked with simulating a moving load in various transverse lane positions.

As observed from NCHRP Project 12-113, the induced axial force in a cross-frame member is highly sensitive to load position relative to the cross-frame panel of interest. For bridges with no support skew, the critical loading position is generally localized about the longitudinal position of the cross-frame (i.e., loads applied 50 feet or more away from the cross-frame result in negligible force effects in the cross-frame member of interest). The governing cross-frame panel will typically be near the location of maximum dead load moment (i.e., midspan for single spans and interior span of continuous units; about 0.35L to 0.40L from the end support in exterior spans of continuous units). In contrast, the load influence in skewed and curved bridges is more variable, especially for cross-frames near end and intermediate skewed supports. For this reason, an influence-surface analysis, or an equivalent method, is required to ensure the critical load position is captured in accordance with Article 3.6.1.4.3.

To satisfy this requirement, an influence-surface grid of 5 feet (longitudinal) by 4 feet (transverse) has been shown to adequately capture the maximum force effects (although a more refined grid could also be implemented). The results of this analysis are summarized in the next section.

Force Effects

The following sections outline the development of design force effects for the following load cases: wind on structure, construction, stability bracing, dead, and live loads. For the sake of clarity, only force effects on a single, critical cross-frame are reported. Note that, in the original design example, the critical member was established as a diagonal in the cross-frame panel at an interior support. Given that the focus of the study is intermediate cross-frames and not support cross-frames (which are designed to transmit lateral deck forces into the bearings), the calculations herein are based on the following critical member: diagonal in an end bay near the maximum positive dead load moment region of the end span.

Wind on Structure

As discussed in a preceding section, force demands in cross-frame elements due to wind are typically determined using hand calculations. Wind pressure acting normal to the bridge fascia should be considered in design during construction and in the final composite system. In the original SBDH Design Example 3 document, wind loads were discussed in general terms, but an explicit design check for cross-frames was not made.

To determine the force demands in the intermediate cross-frames, Article 4.6.2.7 is followed. During construction prior to the composite system, the design wind pressure acting on the fascia girder is distributed longitudinally based on the tributary area associated with the cross-frame spacing. For the curved bridge example here, the tributary width is simply taken as the cross-frame spacing measured along the bridge centerline rather than the chord length or arc length. That effective wind force is then equally distributed to the top and bottom struts of the end-bay cross-frame. Wind loads are then distributed to the adjacent girders through the cross-frame truss systems.

Given that the lateral load is applied to the top and bottom of the X-type cross-frame panel, a portion of the wind load will be resisted by the strut itself (and carried to the next bay) and the remainder is resisted by the diagonal. Conservatively, it is assumed that the diagonal in the end bay resists the full lateral load (and induces a vertical component due to the incline).

In the composite system, wind pressures acting on the upper half of the fascia girder are assumed to be absorbed by the large diaphragm (concrete deck). Wind pressures acting on the lower half of the fascia

girder, however, are conservatively assumed to pass through the end-bay diagonals and into the diaphragm (assuming there is no lateral bracing present). Still, the critical cross-frame member under this loading condition is the diagonal strut in the end bay. Both the construction and final conditions are evaluated herein.

In terms of design loads, the original SBDH example did not discuss design wind pressures. Section 3.8 of AASHTO LRFD has changed considerably since the original design example was published. Considering that wind load provisions are not the primary focus of this design example, 50 psf is adopted as the Strength III design pressure in the final bridge without further investigation to match Design Example 2A. To remain consistent with Table 3.8.1.1.2-1, the Strength V wind pressure is taken as 50 psf multiplied by the squared ratio of (80 mph / 115 mph), or 24 psf.

Design construction pressures are typically limited to due to wind restrictions during steel erection and deck casting. Construction activity is generally limited to 20 mph wind speeds, which corresponds to approximately a 2-psf wind pressure. The process for determining the effective wind force acting on the critical diagonal is similar for construction conditions and the final bridge structure. A sketch is provided, representing wind loading during construction. Relevant design pressure and cross-frame spacing are outlined below. Note that the depth of fascia is conservatively taken as the maximum depth of the nonprismatic, steel girder.

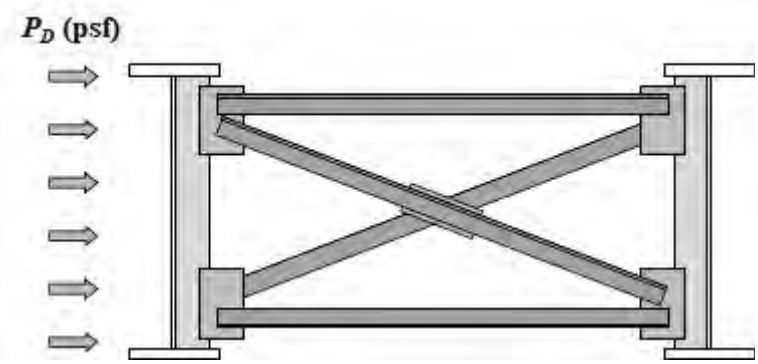

Figure 3: Schematic of wind load applied to the fascia girder

Design pressure, Strength III:	$P_{D.str3} := 50\ psf$
Design pressure, Strength V:	$P_{D.str5} := 24\ psf$
Design pressure, Construction:	$P_{D.c} := 2\ psf$
Unbraced length; critical cross-frame spacing:	$L_b := 20\ ft$
Depth of fascia:	$d := 89.5\ in$

Following Article 4.6.2.7, the process for determining the design force in the critical struts is similar for all construction stages and limit states. The process is summarized with the calculations below. Note that these values represent the compression force (reported as negative value) acting on the governing top or bottom node of the cross-frame panel in the end bay nearest to the fascia subjected to the windward pressures.

Effective strut load, Strength III:	$P_{w.str3.st} := -P_{D.str3} \cdot L_b \cdot \frac{d}{2} = -3.7\ kip$
Effective strut load, Strength V:	$P_{w.str5.st} := -P_{D.str5} \cdot L_b \cdot \frac{d}{2} = -1.8\ kip$
Effective strut load, Construction:	$P_{w.c.st} := -P_{D.c} \cdot L_b \cdot \frac{d}{2} = -0.15\ kip$

As documented above, these effective loads along the bottom flange are conservatively assumed to be resolved entirely about the end-bay diagonal. Thus, the incline geometry of the diagonal must be established to estimate the vertical force component. Girder spacing and brace height are taken directly from the original

design example, except that the brace height is now taken as the girder depth minus 6 inches at the top and bottom (to allow for gusset plate detailing).

Girder spacing: $s_g := 132\ in$

Height of cross-frame brace: $h_b := 72\ in$

Length of diagonal: $L_d := \sqrt{h_b^{\,2} + s_g^{\,2}} = 150.36\ in$

Using statics, the effective diagonal forces are determined. These unfactored forces are subsequently factored later in the load combinations and limit states discussion.

Effective diagonal load, Strength III: $P_{w.str3} := P_{w.str3.st} \cdot \left(\frac{L_d}{s_g}\right) = -4.2\ kip$

Effective diagonal load, Strength V: $P_{w.str5} := P_{w.str5.st} \cdot \left(\frac{L_d}{s_g}\right) = -2\ kip$

Effective diagonal load, Construction: $P_{w.c} := P_{w.c.st} \cdot \left(\frac{L_d}{s_g}\right) = -0.17\ kip$

Overhang Construction

Similar to wind loads, overhang construction loads are typically computed by simple hand methods. To resist the external torque applied to the fascia girders, cross-frames distribute the vertical and horizontal loads on the girders, as well as provide a support for out-of-plane bending of the flanges (i.e., mitigate lateral flange stress effects). The original SBDH Example 3 document calculated overhang loads to evaluate the lateral bending stresses induced in the fascia girder flanges only. In this extended calculation, those same loads are used to calculate the force demands in the cross-frame elements.

In the original design example, the various self-weight and construction loads were identified and quantified. The self-weight components represent the overhanging portion of the wet concrete deck. The construction loads represent the overhang deck forms, the screed rail, a protection railing, a walkway, and the finishing machine. All loads were presented as vertical line loads acting at an offset distance from the vertical plane of the fascia girder, including the moving finishing machine. The summation of the vertically applied loads are summarized below. Due to the assumed incline of the bracket, a horizontal force couple is also imparted on the fascia girder, which is discussed below. A sketch from the original calculation is provided for reference.

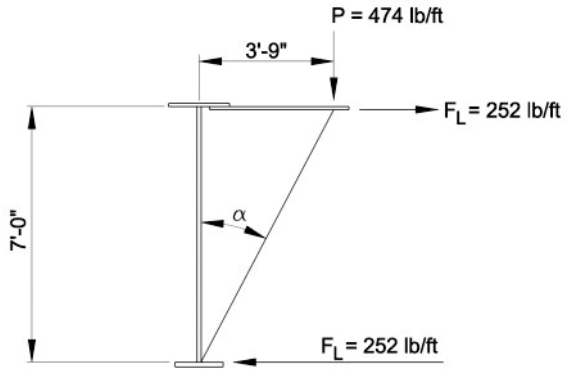

Figure 4: Schematic of construction overhang loads applied to the fascia girder

Uniform load, structure weight: $w_{oh.str} := 234\ plf$

Uniform load, construction weight: $w_{oh.c} := 240\ plf$

Concentrated load, construction weight: $P_{oh.c} := 0\ lbf$

Overhang bracket incline angle: $\alpha := 28\ deg$

These vertical and horizontal loads are assumed to be distributed to each cross-frame line based on a tributary area. In other words, the line loads are multiplied by the spacing between each intermediate cross-frame. The horizontal load component acting laterally on the girder flanges is determined by applying basic principles of statics on the inclined overhang bracket. The lateral force acting on the bottom flange is more critical, as it induces a compression force in the corresponding cross-frame diagonal member. The vertical component of the load, which could potentially introduce differential vertical displacement in the adjacent girders, would induce a tensile force in the same diagonal member, thereby counteracting the compression component from the lateral load. As such, the vertical component is conservatively assumed to be resisted entirely by girder shear such that no additional forces and deformations are imparted on the cross-frame member of interest.

Thus, the force in the critical cross-frame diagonal member is computed by resolving only the horizontal component of the applied load along the member incline. The lateral force component, as noted previously, is conservatively assumed to be resisted entirely by the end-bay diagonal member. This procedure is demonstrated below. Note that the self-weight and the temporary construction loads are computed separately because each are assigned a different load factor later in the calculation set. Recall that compression loads are reported as negative values.

Effective diagonal load, structure weight:

$$P_{oh.str} := -w_{oh.str} \cdot L_b \cdot \tan(\alpha) \cdot \left(\frac{L_d}{s_g}\right) = -2.8\ kip$$

Effective diagonal load, construction weight:

$$P_{oh.c} := -\left(w_{oh.c} \cdot L_b + P_{oh.c}\right) \cdot \tan(\alpha) \cdot \left(\frac{L_d}{s_g}\right) = -2.9\ kip$$

Stability Bracing - Strength

As introduced above, cross-frames are intended to brace longitudinal girders during construction and in the final constructed state. In order to adequately brace girders from out-of-plane buckling, braces must provide adequate strength and stiffness. Braces can either be categorized as lateral braces (preventing out-of-plane lateral movement of the compression flange) or torsional braces (preventing relative twist of the cross-section about its shear center). The most common form of bracing in steel I-girder bridges are cross-frames, since they control girder twist at discrete locations along the length (i.e., torsional braces).

Currently, AASHTO *LRFD* 9th Edition provides no guidance on how to properly design and detail cross-frames to serve as braces. As part of NCHRP Project 12-113, many of the provisions documented in Appendix 6.3 of the AISC Specifications (2016) were evaluated for their implementation into AASHTO. In particular, the torsional brace stiffness and strength requirements were studied for common bridge systems. The calculations herein demonstrate the proposed modifications to these AISC provisions. As previously noted, stability bracing forces could have also been determined from a large-displacement analysis considering initial imperfections. For simplicity, the design expressions proposed for implementation into AASHTO *LRFD* are used.

First, the required strength of the torsional brace is calculated. In other words, the force imparted on the cross-frame as the girder approaches its critical buckling moment is computed. Note that a separate check will be provided later to investigate the required stiffness of the cross-frame to serve as a brace. The required strength of a point, torsional brace is computed by the following equation:

$$M_{br} := \frac{0.036\ M_r \cdot \boldsymbol{L}}{n \cdot C_b \cdot L_b}$$

This equation is based on the findings Liu and Helwig (2020a). Current 15th Edition AISC Specifications (2016) require a brace moment equivalent to 2% of the factored flexural moment in the girder span, which is

independent of the bracing scheme of the girder. Liu and Helwig (2020a) showed that brace moment typically exceeds 2% of the girder moment. Thus, for implementation into AASHTO *LRFD*, it was proposed to adopt the equation above, which is a similar form to the equation presented in the 14th Edition of AISC (2010).

The required brace strength is based on an assumed critical imperfection of L_b/500, where the compression flange has a lateral sweep at the critical brace location and the tension flange remains straight (Han and Helwig, 2020). The original 14th Edition AISC equation is derived from the assumption that twice the ideal torsional stiffness is required to limit the out-of-plane deformations incurred at the critical buckling load. Liu et al. (2020b) demonstrated that three times the ideal stiffness is more appropriate for beam buckling applications. As such, the equation above modifies the AISC (2010) equation to consider a cross-frame stiffness equivalent to three times the ideal stiffness. Hence, the constant is increased from 0.024 to 0.036.

As noted in the NCHRP 12-113 final report, bracing strength requirements are critical for the noncomposite condition of the bridge (i.e., during construction). In the composite system, lateral-torsional buckling of the longitudinal girders is generally not critical at the intermediate support due to the restraint provided by the bearings and concrete deck. The bearings and deck provide restraint to twisting of the cross-section even in systems where shear studs are omitted in the negative moment region. In the negative moment regions of continuous systems, web distortional buckling, which is not significantly affected by the unbraced length, is much more critical than conventional LTB, particularly for slender unstiffened webs (Helwig and Yura, 2015). Web distortional effects, although important to girder design, are not evaluated in this calculation set.

With these factors in mind, these bracing requirements are evaluated at all critical stages of construction. In this example, the critical stage for stability bracing is during deck construction before the concrete has cured. The deck forms provide no buckling restraint to the girders, such that the cross-frames are the sole source of stability bracing (assuming no temporary, external bracing mechanisms are provided by the erector). Although only one stage of construction is explicitly considered in this example, it is important to examine all potentially critical stages, particularly those where permanent bracing is not fully installed and girders may be subjected to long unbraced lengths. For all construction stages examined, it is imperative that the the appropriate M_r term in the bracing strength equation is considered. Additionally, only load cases that act concurrently with the critical construction stage should be considered in the load combination. For instance, overhang deck construction loads need not be combined with stability bracing forces corresponding to intermediate phases of steel erection, as these conditions are not concurrent.

As such, the focus of this design example is related to stability bracing demands directly after the deck is cast and the concrete is still wet. To satisfy the bracing strength requirements, both the critical positive and negative moment regions must be evaluated for this continuous span. This is achieved by designing all cross-frame braces in the span for the maximum value of M_r/C_bL_b. For this example, two different unbraced segments are checked: the one containing the maximum positive moment and the one containing the maximum negative moment (i.e., the end segment).

Before presenting those calculations, it should be noted that the L_b value to consider need not be taken less than the maximum unbraced length permitted for the beam to reach the required flexural strength, M_r. This provision accounts for scenarios in which the spacing of the brace is significantly less than is required to develop the required strength of the beam. In essence, this provision lessens the demands on cross-frames for girders that would not buckle under the specified cross-frame layout (i.e., the girder would partially or fully yield prior to buckling). In this particular example, the end segment has an unbraced length of 20 feet, which is close to L_p, the limiting unbraced length to achieve the nominal resistance of the girder cross-section under uniform bending. Thus, it is evident that increasing the L_b value in the denominator of the equation above is warranted, as this segment (although subjected to the largest moment magnitude) is controlled by yielding and not LTB. This is demonstrated below.

Lastly, because the individual spans of this bridge have different lengths, L, and number of intermediate braces, n, these design checks shall be performed for each span. However, given that the critical cross-frame

member of interest is in the 160-foot end span, only bracing forces corresponding to those span conditions are computed herein.

First, the critical unbraced segment in the positive moment region is checked. In this particular instance, the girder moment is taken as the maximum positive moment caused by DC1 loads (i.e., the dead loads acting concurrently with the critical stage of construction considered). Because the force demands on cross-frames are evaluated on the outer girder (max radius) which is critical during deck construction, the DC1 girder moments, taken directly from Table 8 of the original document, are used for this calculation. Note that similar girder forces were determined from the 3D model developed for obtaining dead and live load cross-frame forces.

The M_r term in the equation is based on the factored girder moment. Because two different limit states and load combinations were evaluated that consider stability bracing requirements, these bracing forces are subsequently factored later in the calculation set. Thus, the required brace moment is presented as an unfactored magnitude for now.

Span length: $L := 160\ ft$

Number of intermediate braces: $n_b := 7$

Maximum girder moment in segment: $M_r := 3453\ kip \cdot ft$

The L_b term to consider, as noted above, need not be taken less than the maximum unbraced length permitted for the beam to develop its required flexural strength, M_r. As such, Article 6.10.8.2.3 was utilized to determine the maximum unbraced length that the positive-moment girder segment could have, for which its LTB capacity still exceeds the required strength (taken as 1.4 times M_r, or 4834 k-ft, to represent the critical construction load combination outlined below). Considering the steel section properties only (i.e., no composite properties for this stage of construction) and taking C_b as 1.0, it was determined that the maximum L_b value is almost 45 feet. These calculations are presented below for reference.

Many of the notable parameters, including the effective radius of gyration for LTB and the web load-shedding factor, are taken directly from the original design calculation. Eq. 6.10.8.2.3-3 in AASHTO LRFD, the elastic LTB expression which conservatively neglects the torsion constant term, is rearranged in such a way that the L_b required to equate the required strength and applicable LTB capacity can be computed. Note that the moment gradient factor was conservatively taken as unity to simplify the calculation. As L_b increases, C_b slightly changes but is generally not much larger than 1.0.

Moment gradient factor: $C_b := 1.0$

Web load-shedding factor: $R_b := 1.0$

Effective radius of gyration for LTB: $r_t := 4.81\ in$

Section modulus, top compression flange: $S_{xc} := 2477\ in^3$

Modulus of elasticity, steel: $E := 29000\ ksi$

Maximum permissible unbraced length to develop maximum positive girder moment (4834 kip-ft):

$$L_b := \sqrt{\frac{C_b \cdot R_b \cdot \pi^2 \cdot E \cdot r_t^{\,2} \cdot S_{xc}}{1.4\ M_r}} = 44.3\ ft$$

Lastly, the C_b term used in the brace strength equation, despite the discussion above for computing the appropriate unbraced length, is based the moment gradient factor in the actual unbraced segment. Calculations show, however, that C_b is nearly unity for the specified 20-foot unbraced segment and the moment diagram above. Therefore, it conservatively taken as 1.0.

Moment gradient factor: $C_b := 1.0$

With each parameter established, the required torsional brace strength for the positive-moment segment is given by the following:

$$M_{br.pos} := \frac{0.036\ M_r \cdot L}{n_b \cdot C_b \cdot L_b} = 64.1\ \textit{kip} \cdot \textit{ft}$$

Now, the critical unbraced segment in the negative moment region is checked. In this case, the maximum girder moment is taken as the maximum negative moment caused by DC1 loads (i.e., the dead loads acting concurrently with the critical stage of construction considered).

Maximum moment in girder moment (unfactored): $M_r := 9189\ \textit{kip} \cdot \textit{ft}$

Similar to the procedure outlined above, Article 6.10.8.2.3 was utilized to determine the maximum unbraced length for the critical negative-moment girder segment. The notable differences between the positive and negative moment calculations are the girder section properties used (i.e., the web and flange dimensions are larger in the negative moment region) and the moment gradient factor. To simplify the calculations, C_b was conservatively taken as 1.8. Again, C_b slightly changes as L_b increases, but a conservative estimate of the moment gradient factor for this reverse-curvature bending was 1.8. For reference, a moment gradient factor of 1.67 corresponds to a straight-line moment diagram where the one end of the unbraced segment has zero moment to represent an inflection point for the moment diagram of the entire span. With those factors in mind, it was determined that the maximum L_b value is nearly 97 feet which is substantially larger than the actual unbraced length of 20 feet. These calculations, which are similar to those presented above for the positive moment region, are not presented herein.

Maximum permissible unbraced length to develop maximum negative girder moment (1.4 x 9189 kip-ft): $L_b := 97\ \textit{ft}$

Despite the discussion above, the C_b factor corresponding to the actual 20-foot unbraced segment and moment diagram is approximately 1.23 using AISC Specifications guidance (Equation F1-1).

Moment gradient factor: $C_b := 1.23$

Thus, the required torsional brace strength for the negative moment region segment is given by the following:

$$M_{br.neg} := \frac{0.036\ M_r \cdot L}{n_b \cdot C_b \cdot L_b} = 63.4\ \textit{kip} \cdot \textit{ft}$$

For simplicity, the same cross-frame size is used throughout. Therefore, the appropriate brace moment, for which all cross-frames in the span would be designed, is the largest of the two segments presented above.

$$M_{br} := \max\left(M_{br.pos}, M_{br.neg}\right) = 64.1\ \textit{kip} \cdot \textit{ft}$$

The torsional brace moment is then converted into a force couple acting at the top and bottom of the cross-frame trusswork. Provided that a girder can buckle out of plane in either direction depending on the nature of its imperfections, the sign of the force couple can vary. In terms of the bottom strut design throughout this calculation set, a compression load is more critical. Therefore, the unfactored force demand due to stability bracing is taken as the value below in terms of compression (reported as negative value) assuming a compression-diagonal system (as opposed to a tension-only diagonal system). This force effect will be appropriately factored and combined with wind and construction loads at the end of the calculation set. This is demonstrated schematically in the figure below.

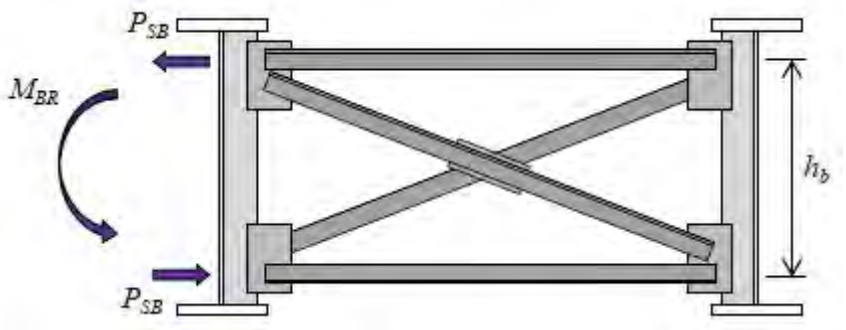

Figure 5: Schematic demonstrating the development of stability bracing forces in cross-frames

Height of cross-frame brace: $h_b = 72\ in$

$$P_{sb} := -\frac{M_{br}}{h_b} \cdot \left(\frac{L_d}{s_g}\right) = -12.2\ kip$$

Dead Load

As documented extensively in Article 6.7.2 and its associated commentary, there are two different types of dead load forces that act on a cross-frame throughout its life: the internal dead load forces and the "fit-up" forces, which are external forces that the erector may need to apply to assemble the structural steel during erection. The fit-up forces are largely dependent on which fit condition is selected by the engineer and built by the steel erector. The three most common fit conditions are: (i) no-load fit (NLF), (ii) steel dead load fit (SDLF), and (iii) total dead load fit (TDLF). The original SBDH example specified a NLF, such that the girders are assumed plumb when cross-frames are installed (i.e., steel framing erected on the ground). Therefore, the external forces required to fit the cross-frames are assumed negligible. With that in mind, only the internal dead load forces developed during construction are considered in the design of the cross-frames in this example. For different fit conditions particularly in skewed and/or curved bridges, refer to Article 6.7.2 or NCHRP 20-07/Task 355 (White et al. 2015) for refined analysis techniques and simplified methods for estimating these locked-in force effects.

Noncomposite girders in curved bridges typically experience differential deflection, and twist of the cross-section can be significant. Thus, the internal dead load forces due to construction and self-weight material loads are typically substantial when compared to those in straight bridges with normal supports. A refined 3D analysis model was developed to capture the effects of staged construction.

Internal dead load force effects in cross-frames under the NLF assumption are essentially determined by applying and combining gravity loads at every stage of construction: steel erection, installing formwork, deck casting (staged or simultaneous pour), barrier casting, and wearing surface pour. This procedure was performed in the 3D model introduced previously. To remain consistent with the original design example, two different deck pour scenarios were considered: (i) a five-pour scheme as demonstrated by Figure 4 in the original SBDH example and (ii) a continuous single pour scheme. Ultimately, the design loads are governed by the more critical scenario.

The following steps below outline the dead load forces due to all intermediate stages of construction. They are organized and designated as DC1 (dead loads applied to the noncomposite system), DC2 (dead loads applied to the composite system), and DW (wearing surface loads applied to the composite system). To remain consistent with the wind and overhang loads described above, only the most critical diagonal member in the outer-radius end bay is checked. As expected, the most critical diagonal member was found to occur at in the maximum dead load moment region where girder deflections are greatest (i.e., approximately 0.35L measured from the end support). Note that, although not explicitly presented here, similar calculations are to be made for other cross-frame members that may govern the design.

In terms of DC1 loads, the self-weight of the steel framing, the stay-in-place deck forms, and the concrete deck (including haunch and overhangs) were considered. These loads are assumed to act on the noncomposite system (or steel section alone). Deck forms were assumed to weigh 15 psf in accordance with the original design example. From a staged construction analysis, the following DC1 force effects were provided by the 3D analysis model for the critical cross-frame diagonal member:

Dead load, steel framing: $P_{dc.s} := -2.33\ kip$

Dead load, formwork: $P_{dc.f} := -1.40\ kip$

Dead load, wet concrete deck: $P_{dc.d} := -8.97\ kip$

Therefore, the combined DC1 force effect in the critical diagonal member is as follows (all loads in compression):

$$P_{dc1} := P_{dc.s} + P_{dc.f} + P_{dc.d} = -12.7\ kip$$

DC2 loads, in this case, are comprised solely of barrier loads since the bridge is assumed to have no sidewalks and medians. The barrier weight is taken as 495 plf to replicate the original design example. When performing hand calculations, barrier loads are often distributed equally to all girders across the width. In the refined analysis model, each barrier load is applied at a 1-foot offset distance from the deck edge, and the model distributes the load based on stiffness in accordance with Article C4.6.1.2.4b. The load is applied to the long-term composite structure. The following DC2 force effect was determined for the critical diagonal member:

$$P_{dc2} := 3.24\ kip$$

Future wearing surface loads, like DC2 loads, are assumed to act on the long-term composite system and are typically distributed equally to all girders in hand calculations. Applying a 30 psf load to the deck and running the analysis model, the following DW force effect was determined for the critical diagonal member:

$$P_{dw} := -2.54\ kip$$

It is evident from the magnitudes of these loads that dead load effects on cross-frames in curved bridges are not insignificant as is commonly observed in straight bridges with normal supports. The wet concrete load produces the highest force effects. The force effects outlined above are appropriately factored and combined with wind, construction, stability bracing, and live loads later in the calculation set.

Live Load and Impact

Similar to dead loads, live load force effects are determined from the 3D analysis model. The influence-surface procedure outlined previously was performed. The result of the influence-surface analysis is a color contour plot, which demonstrates the axial-force response of the select diagonal cross-frame member due to a 1-kip load positioned at a given spatial coordinate on the deck surface. For the member of interest, the corresponding contour plot is presented below for reference.

For loads applied in the "red" area on the plot, the compression force in the diagonal is maximized. For loads in the "blue" area, the tension force in the diagonal is maximized. Load positions in grey have negligible influence on the axial-force response in that cross-frame. In terms of design loads, the strength and fatigue limit states are handled differently. For the strength limit state, loads in accordance with Article 3.6.1.3 were applied. For the fatigue limit state, loads in accordance with Article 3.6.1.4 were applied. The commercial software package was utilized to apply these separate loading conditions, and the results were validated with hand solutions. To demonstrate one example, the influence-line response of the diagonal member due to the AASHTO fatigue truck is presented below. In this example, the fatigue truck traverses the length of the bridge (left to right orientation in influence surface) with its transverse centerline directly over the bridge centerline. This process was repeated for all transverse lane positions in both the forward and backward

directions to ultimately find the governing force demands.

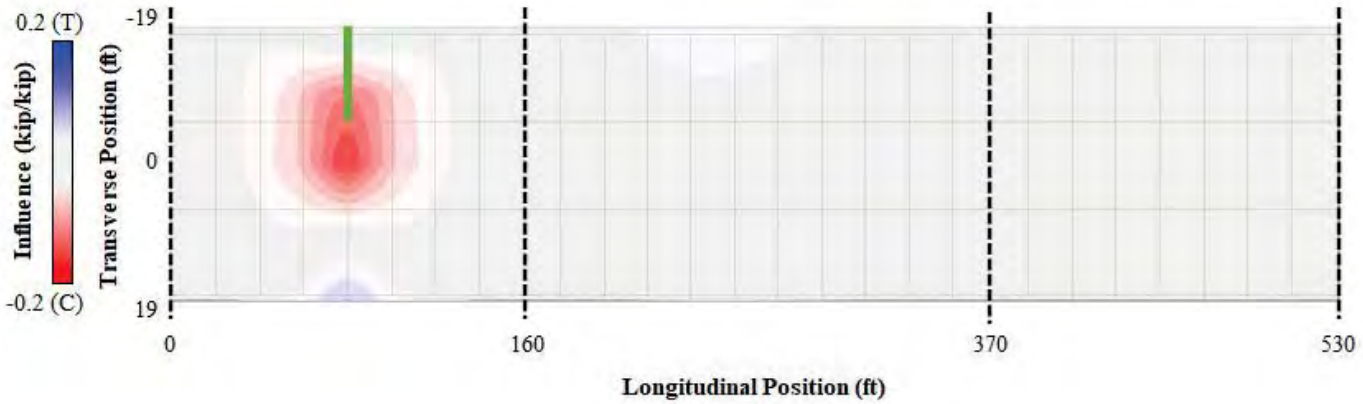

Figure 6: Influence-surface plot generated for the critical cross-frame member

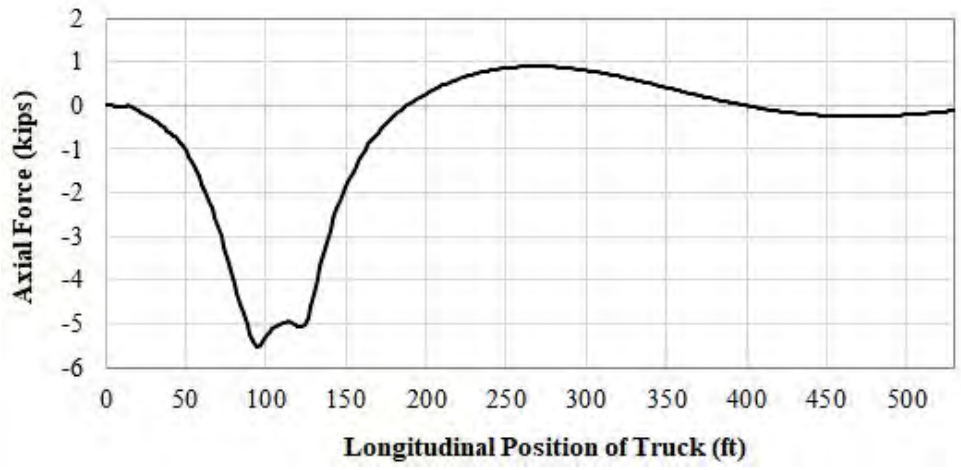

Figure 7: Sample influence-line plot generated for the critical cross-frame member

The force effects below summarize the output from the 3D analysis model that made use of the loading conditions outlined in Article 3.6.1.3 (strength) and Article 3.6.1.4 (fatigue). Note that for the strength limit state, the maximum tension and compression forces are recorded; for the fatigue limit state, the critical total force range is recorded. The critical force range for fatigue was determined based on Article C6.6.1.2.1 (i.e., any stress/force cycle that has a tensile component). Note that the appropriate impact factors are also included in the reported results. An dynamic load allowance factor of 0.33 is applied to the design truck or tandem in the strength limit state, and a factor of 0.15 is applied to the truck in the fatigue limit state. The force effects below will be appropriately factored and combined with wind, construction, stability bracing, and dead loads later in the calculation set.

Live load, strength envelope: $P_{ll.str.t} := 8.50\ kip$

$P_{ll.str.c} := -23.65\ kip$

Live load, fatigue force range: $P_{ll.fat} := 7.27\ kip$

Limit States and Load Combinations

Now that the unfactored design loads have been established for the critical cross-frame diagonal member, a discussion on the applicable limit states is warranted. Tables are provided below that identify the appropriate load combinations and load factors to consider. Each of these items is discussed below in the context of cross-frame design.

Following Articles 3.4.1 and 3.4.2, the adequacy of the cross-frames must be evaluated during all

construction stages and in the final constructed state using the load combinations in Table 3.4.1-1. Strength I, Strength III, Strength V, Fatigue I, and Fatigue II are specifically addressed. Aside from the main load combinations, there are three additional items to note. First, Article 3.4.2 introduces special combinations for construction loads, which are considered herein. Second, despite not being explicitly considered in Table 3.4.1-1, stability bracing force effects shall also be considered based on the proposed specification language in Article 3.4.2. Note that the stability bracing load factors are marked with an asterisk in the table below because these force effects are not independently factored. Instead, they are based on the corresponding factored girder moment. Third, the cross-frame-specific load factors proposed as part of NCHRP 12-113 are also included. These values are signified with a double asterisk in the table.

Recall that the following load cases have been evaluated above: dead load (DC1, DC2, DW), live load (strength LL, fatigue LL), overhang construction (CL), wind on structure (construction WS, final WS), and stability bracing (SB). During construction, the critical stage consists of the noncomposite system immediately after deck casting (i.e. wet concrete load). For this condition, two limit states and load combinations have been identified as critical: Strength III and the special construction case. These load combinations are tabulated below:

	DC1	DC2	DW	LL+IM	$(LL+IM)_f$	WS	CL	SB
Strength III	1.25	–	–	–	–	1.25	1.5	*
Construction	1.4	–	–	–	–	–	1.4	*

In the finished bridge when DC2, DW, and LL cases are introduced, additional limit states and combinations are investigated, which are tabulated below.

	DC1	DC2	DW	LL+IM	$(LL+IM)_f$	WS	CL	SB
Strength I	1.25	1.25	1.5	1.75	–	–	–	–
Strength III	1.25	1.25	1.5	–	–	1	–	–
Strength V	1.25	1.25	1.5	1.35	–	1	–	–
Fatigue I	–	–	–	–	1.14**	–	–	–
Fatigue II	–	–	–	–	0.52**	–	–	–

With the limit states established, the next step is to determine the factored combined force effects for the cross-frame member of interest. Note that the ductility factor (Article 1.3.3), the redundancy factor (1.3.4), and the operational importance factor (1.3.5) are all taken as 1.0 in this example. First, the construction-related loads are summarized:

DC1, vertical loads: $P_{dc1} = -12.7$ ***kip***

DC1, overhang loads: $P_{oh.str} = -2.83$ ***kip***

WS, construction: $P_{w.c} = -0.17$ ***kip***

CL, overhang loads: $P_{oh.c} = -2.91$ ***kip***

SB: $P_{sb} = -12.17$ ***kip***

Strength III limit state, construction:

$$P_{c.str3} := 1.25 \cdot \left(P_{dc1} + P_{oh.str}\right) + 1.25 \cdot P_{w.c} + 1.5 \cdot P_{oh.c} + 1.25 \cdot P_{sb} = -39.2 \text{ kip}$$

Construction condition:

$$P_{c.cl} := 1.4 \cdot \left(P_{dc1} + P_{oh.str}\right) + 1.4 \cdot P_{oh.c} + 1.4 \cdot P_{sb} = -42.9 \text{ kip}$$

Next, the load combinations corresponding to the finished bridge are summarized. Ultimately, compression forces will govern over tension forces for cross-frame single-angle design (except for the fatigue limit state); thus, only the maximum live load induced compression force is presented.

LL+IM (Strength): $P_{ll.str.c} = -23.65$ ***kip***

LL+IM (Fatigue): $P_{ll.fat} = 7.27\ kip$

WS, finished (Strength III): $P_{w.str3} = -4.25\ kip$

WS, finished (Strength III): $P_{w.str5} = -2.04\ kip$

Strength I limit state:

$$P_{str1} := 1.25 \cdot \left(P_{dc1} + P_{dc2}\right) + 1.5 \cdot P_{dw} + 1.75 \cdot P_{ll.str.c} = -57\ kip$$

Strength III limit state:

$$P_{str3} := 1.25 \cdot \left(P_{dc1} + P_{dc2}\right) + 1.5 \cdot P_{dw} + 1.0 \cdot P_{w.str3} = -19.9\ kip$$

Strength V limit state:

$$P_{str5} := 1.25 \cdot \left(P_{dc1} + P_{dc2}\right) + 1.5 \cdot P_{dw} + 1.35 \cdot P_{ll.str.c} + 1.0 \cdot P_{w.str5} = -49.6\ kip$$

Fatigue I (infinite life) limit state:

$$P_{f1} := 1.75 \cdot 0.65 \cdot P_{ll.fat} = 8.3\ kip$$

Fatigue II (finite life) limit state:

$$P_{f2} := 0.8 \cdot 0.65 \cdot P_{ll.fat} = 3.8\ kip$$

Therefore, the governing force demands for the strength and fatigue limit states are summarized below (compression forces taken as negative values). Note that the construction stage governs the strength design of the cross-frame of interest. The appropriate fatigue limit state (Fatigue I or II) is determined in the subsequent section.

Strength limit state:

$$P_{str} := -\max\left(\left|P_{c.str3}\right|, \left|P_{c.cl}\right|, \left|P_{str1}\right|, \left|P_{str3}\right|, \left|P_{str5}\right|\right) = -57\ kip$$

Fatigue I (infinite life) limit state:

$$P_{f1} = 8.3\ kip$$

Fatigue II (finite life) limit state:

$$P_{f2} = 3.8\ kip$$

It is important to note that these factored loads are smaller than the original design example for three primary reasons. First, the original example did not incorporate the cross-frame stiffness modification factor, *R*, into the analysis model. Second, the original example examined a cross-frame diagonal at an intermediate support, whereas this example examined a diagonal near the maximum positive dead load moment region of the end span. Third, older versions of AASHTO *LRFD* required designers to consider a double-truck fatigue load case, which produced large force ranges despite the relative infrequence of that loading scenario. This has since been removed from the code and verified through NCHRP 12-113.

Resistance

The following section outlines the development of factored resistances for the critical single-angle diagonal member. Strength and fatigue limit states are addressed separately.

Strength Limit State

The original SBDH example problem provided a detailed calculation of the compressive resistance of the diagonal cross-frame member, which is still applicable to the design example. For completeness, the same calculations are provided with several exceptions, as noted herein. In general, the calculations compute the factored resistance of a L8x8x3/4 single angle member eccentrically loaded in compression with a 1/2-inch thick connection plate, as well as perform appropriate slenderness checks. The following parameters characterize the cross-section properties of the angle based on Table 1-7 in the AISC Manual (2017).

Gross area of angle: $A_g := 11.40\ in^2$

Radius of gyration, z-axis: $r_z := 1.57\ in$

Radius of gyration, x-axis: $r_x := 2.46\ in$

Radius of gyration, y-axis: $r_y := 2.46\ in$

Leg width: $b := 8.0\ in$

Leg thickness: $t := 0.75\ in$

Steel material properties are summarized below. Note that grade 50 steel is assumed for the cross-frame elements.

Modulus of elasticity, steel: $E = 29000\ ksi$

Yield strength: $F_y := 50\ ksi$

Next, the slenderness of the outstanding legs (Article 6.9.4.2.1) and the global member slenderness (6.9.3) must be checked. The plate buckling coefficient is taken as 0.45 per Table 6.9.4.2.1-1.

Slenderness of cross-section: $\frac{b}{t} = 10.7$

Plate buckling coefficient: $k := 0.45$

Slenderness limit: $\lambda_r := k \cdot \sqrt{\frac{E}{F_y}} = 10.8$

$$Check := \left\| \begin{array}{l} \text{if } \frac{b}{t} > \lambda_r \\ \quad \| \text{“Slender section”} \\ \text{else} \\ \quad \| \text{“Nonslender section”} \end{array} \right| = \text{“Nonslender section”}$$

Since the section is deemed nonslender, Article 6.9.4.2.2 need not be checked. The slenderness provision of Article 6.9.3, though, must also be evaluated. Since the member is considered a primary member, the slenderness limit is set as 120. The unbraced length of the single-angle diagonal is conservatively taken as the *Ld* term computed above (i.e., neglecting the connection and gusset plates). The effective length factor is then taken as 1.0 for single members per Article 4.6.2.5.

Effective length factor: $K := 1.0$

Unbraced length: $l := L_d = 150.4\ in$

Minimum radius of gyration: $r_{min} := r_z = 1.57\ in$

Slenderness of member: $\frac{K \cdot l}{r_{min}} = 95.8$

$$Check := \left\| \begin{array}{l} \text{if } \frac{K \cdot l}{r_{min}} > 120 \\ \quad \| \text{“Slender; revisit design”} \\ \text{else} \\ \quad \| \text{“OK”} \end{array} \right\| = \text{“OK”}$$

Having satisfied the basic slenderness provisions, the angle must now be checked for the strength limit state in accordance with Article 6.9.4.4. The cross-frame member of interest, like many single angle sections, is eccentrically loaded due to the connection to the gusset plate through one leg only. Therefore, the member is subjected to axial and flexural stresses, which complicates the calculation of compression resistance. Article 6.9.4.4 employs a simplified approach to computing the resistance. The bending moments are effectively neglected in lieu of assigning an effective slenderness ratio for flexural buckling. Also, per Article 6.9.4.4, single angles designed using this simplified procedure need not be checked for flexural-torsional buckling. The calculation of the effective slenderness ratio is presented herein (for equal-leg angles).

Effective slenderness:

$$\lambda_{eff} := \left\| \begin{array}{l} \text{if } \frac{l}{r_x} \le 80 \\ \quad \| 72 + 0.75 \cdot \frac{l}{r_x} \\ \text{else} \\ \quad \| 32 + 1.25 \cdot \frac{l}{r_x} \end{array} \right\| = 117.8$$

With the effective slenderness ratio known, Article 6.4.1.1 can be enforced to compute the compression resistance of the member. The nominal resistance is calculated as follows:

Elastic critical buckling resistance:

$$P_e := \frac{\pi^2 \, E}{(\lambda_{eff})^2} \cdot A_g = 235 \ \textit{kip}$$

Nominal yield resistance:

$$P_o := F_y \cdot A_g = 570 \ \textit{kip}$$

Nominal compression resistance:

$$P_n := \left\| \begin{array}{l} \text{if } \frac{P_e}{P_o} \ge 0.44 \\ \quad \| \left(0.6558^{\left(\frac{P_o}{P_e}\right)} \right) \cdot P_o \\ \text{else} \\ \quad \| 0.877 \cdot P_e \end{array} \right\| = 206.1 \ \textit{kip}$$

Therefore, the nominal resistance computed above still applies. Now, the factored resistance is computed per Article 6.5.4.2 and 6.9.2.1.

Resistance factor:

$$\phi_c := 0.95$$

Factored compression resistance:

$$P_{r.str} := \phi_c \cdot P_n = 195.8 \ \textit{kip}$$

The factored compressive resistance is to be compared against the factored force demand determined in the previous section. This check is provided in the subsequent section. Had tensile forces governed the design, refer to Article 6.8 for the appropriate design procedures.

Fatigue Limit State

As suggested in Article 6.6.1.1, both load-induced (6.6.1.2) and distortion-induced (6.6.1.3) fatigue shall be considered in design of cross-frames. For this example, though, it is assumed that the cross-frame and its connection plates are detailed properly in accordance with Article 6.6.1.3 such that distortion-induced fatigue is not a design concern. Therefore, only load-induced fatigue is a design consideration herein. The first step in computing the load-induced fatigue resistance of the single-angle cross-frame member is to establish the fatigue category and its pertinent design parameters. Per Table 6.6.1.2.3-1 (Section 7.2), a single-angle member welded along one side to a connection plate is given the E' designation (McDonald and Frank, 2009). Note that the original example was based on an E detail given the state of the design specification at that time. Therefore, the following parameters are used herein:

Detail category constant: $A := 3.9 \cdot 10^8 \ ksi^3$

Threshold stress: $\Delta F_{th} := 2.6 \ ksi$

Next, the appropriate limit state (Fatigue I versus Fatigue II) must be established. Per Article 6.6.1.2.3, if the projected single-lane Average Daily Truck Traffic (ADTT) is less than or equal to the applicable value in Table 6.6.1.2.3-2, then the member shall be designed for finite-life (Fatigue II). To make that determination, the projected truck traffic on the bridge must be estimated. To maintain consistency with the original SBDH example, a single-lane ADTT of 1,000 trucks per day is assumed. Therefore, the cross-frame detail shall be designed for the Fatigue II limit state, as demonstrated mathematically below.

Single-lane ADTT: $ADTT_{sl} := 1000$

75-year single-lane ADTT equivalent to infinite life: $ADTT_{sl.inf} := 8485$

$$Check := \left\| \begin{array}{l} \text{if } ADTT_{sl} \le ADTT_{sl.inf} \\ \quad \| \text{“Design for Fatigue II”} \\ \text{else} \\ \quad \| \text{“Design for Fatigue I”} \end{array} \right| = \text{“Design for Fatigue II”}$$

Therefore, the nominal fatigue resistance is calculated in accordance with Article 6.6.1.2.5 and Eq. 6.6.1.2.5-2 specifically. To do so, the total number of stress cycles expected on the cross-frame member of interest during the 75-year design span must be computed. This requires an assumption on the number of stress range cycles per truck passage (Table 6.6.1.2.5-2). Based on the findings of NCHRP 12-113, assuming one stress cycle per truck passage for cross-frame members is most appropriate. The calculations are presented below.

Cycles per truck passage: $n := 1.0$

Total design cycles: $N := 365 \cdot 75 \cdot n \cdot ADTT_{sl} = 2.738 \cdot 10^7$

Nominal fatigue resistance: $\Delta F_n := \left(\frac{A}{N}\right)^{\frac{1}{3}} = 2.42 \ ksi$

In accordance with Article C6.6.1.2.2, both the resistance factor and the additional load modifiers are taken as 1.0. Therefore, the factored fatigue resistance is taken as the following. Note that fatigue resistance is typically computed in terms of axial stress (i.e., *P/A*); the factored fatigue force determined above will be converted to stress and compared to the resistance in the subsequent section.

Resistance factor: $\phi_f := 1.0$

Factored fatigue resistance: $\Delta F_r := \phi_f \cdot \Delta F_n = 2.42 \ ksi$

Final Design Check

As outlined previously, a strength and fatigue limit state design check are to be made. The calculations herein simply compile the factored design loads and factored resistances computed in previous sections of the calculation set. Note that Fatigue II design checks are made in terms of stress. As such, the previously determined fatigue forces are converted to axial stress by considering shear lag effects in accordance with Table 6.6.1.2.3-1 (Section 7.2). Note that the weld length was set as 7 inches to maintain consistency with the original example. Although not explicitly demonstrated, similar design calculations must be made for the connections and connecting parts.

Strength Limit State

Factored compression resistance: $P_{r.str} = 195.8\ kip$

Governing factored force: $P_{str} = 57\ kip$ (Compression)

$$Check := \left\| \begin{array}{l} \text{if } P_{r.str} \geq P_{str} \\ \quad \| \text{“OK”} \\ \text{else} \\ \quad \| \text{“N.G.; Refine Design”} \end{array} \right\| = \text{“OK”}$$

Fatigue Limit State

Factored fatigue resistance: $\Delta F_r = 2.42\ ksi$

Governing factored force: $P_{f2} = 3.8\ kip$

Assumed weld length: $L_w := 7\ in$

Distance from single-angle centroid to surface of gusset: $x_{bar} := 2.26\ in$

Shear lag factor: $U := 1 - \frac{x_{bar}}{L_w} = 0.7$

Net effective area: $A_{net} := U \cdot A_g = 7.72\ in^2$

Governing factored stress range: $\Delta f := \frac{P_{f2}}{A_{net}} = 0.49\ ksi$

$$Check := \left\| \begin{array}{l} \text{if } \Delta F_r \geq \Delta f \\ \quad \| \text{“OK”} \\ \text{else} \\ \quad \| \text{“N.G.; Refine Design”} \end{array} \right\| = \text{“OK”}$$

It is apparent that cross-frame member is adequately proportioned for the strength and fatigue limit states, even with the conservative assumption used with the hand calculations (i.e., the diagonal resists the full lateral load instead of distributing the load with the strut member). Based on the demand-to-capacity ratios, it is also apparent that there is significant reserve capacity. Consequently, a smaller angle section than L8x8x3/4 could also be used to improve economy. If the designer chooses to reduce the cross-section, then the 3D analyses would need to be re-run with the updated section to verify the new section is adequate. Recall that the cross-frame forces are directly related to its cross-sectional area given the indeterminacy of the system. For the sake of clarity, this process is not demonstrated in this calculation set.

Stability Bracing - Stiffness

As outlined above and in proposed Article 6.7.4.2.2, braces must be designed to possess adequate strength and stiffness. The strength requirements were previously outlined. In this section, a separate check is provided to evaluate the required stiffness of the cross-frame. Similar to the brace strength requirements, proposed modifications have been made to the 15th Edition AISC provisions on torsional brace design. The proposed expression for the required brace stiffness is given with the following expression:

$$\beta_{T.req} := \frac{3.6\ L}{\phi_{br} \cdot n \cdot E \cdot I_{y.eff}} \cdot \left(\frac{\gamma_{CL} \cdot M_r}{C_b} \right)^2$$

As previously discussed, Liu et al. (2020b) observed that providing three times the ideal stiffness is more appropriate for beam buckling than twice the ideal stiffness, as assumed in the AISC bracing provisions. As such, the AISC equation has been modified by increasing the constant in the numerator by 50% (from 2.4 to 3.6). The following parameters describe the load and resistance factors assumed. Because the braces are evaluated during the critical stage of construction, the load factor associated with the construction condition is adopted here. The resistance factor is taken to match the values provided in AISC Appendix 6.3.

Resistance factor: $\phi_{br} := 0.80$

Load factor: $\gamma_{CL} := 1.4$

Recall the maximum DC1 moment as well as the moment gradient assumption from the brace strength calculation was governed by the positive moment region. As such, these parameters are established again.

Maximum unfactored moment: $M_r := 3453\ \textit{kip} \cdot \textit{ft}$

Moment gradient factor: $C_b := 1.0$

The following parameters describe the cross-section of the girder and the bracing scheme. The girder is nonprismatic, which complicates the buckling behavior. Because the critical brace frames into section G4-1 (notation from original example) of the nonprismatic beam (outer-radius girder), those cross-sectional dimensions are assumed. The distance between the extreme fibers and the neutral axis is computed to determine an effective weak-axis moment of inertia, given that the section is also singly-symmetric.

Number of intermediate braces: $n_b = 7$

Tension flange width: $b_{f.t} := 21\ \textit{in}$

Tension flange thickness: $t_{f.t} := 1.5\ \textit{in}$

Compression flange width: $b_{f.c} := 20\ \textit{in}$

Compression flange thickness: $t_{f.c} := 1\ \textit{in}$

Web depth: $d_w := 84\ \textit{in}$

Web thickness: $t_w := 0.5625\ \textit{in}$

Distance from top fiber to neutral axis:

$$c := \frac{b_{f.t} \cdot t_{f.t} \cdot \frac{t_{f.t}}{2} + d_w \cdot t_w \cdot \left(t_{f.t} + \frac{d_w}{2} \right) + b_{f.c} \cdot t_{f.c} \cdot \left(t_{f.t} + d_w + \frac{t_{f.c}}{2} \right)}{b_{f.t} \cdot t_{f.t} + d_w \cdot t_w + b_{f.c} \cdot t_{f.c}} = 38.471\ \textit{in}$$

Distance from bottom fiber to neutral axis: $t := \left(t_{f.t} + d_w + t_{f.c} \right) - c = 48.029\ \textit{in}$

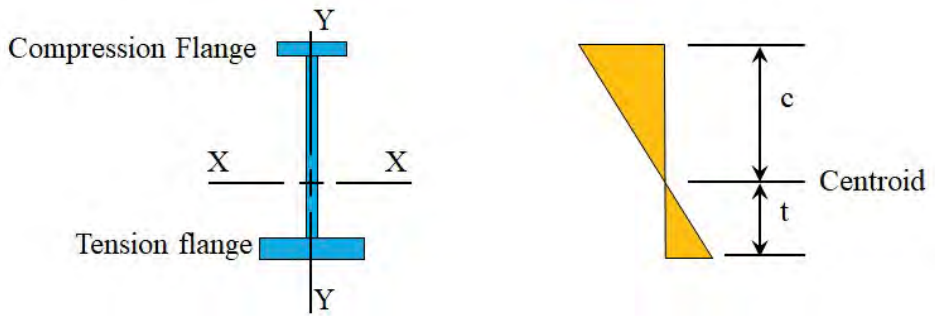

Figure 8: Schematic showing the definition of *c* and *t* variables

Tension flange moment of inertia: $I_{y.t} := \frac{1}{12} \cdot t_{f.t} \cdot b_{f.t}^{\ 3} = \left(1.2 \cdot 10^3\right)\ in^4$

Compression flange moment of inertia: $I_{y.c} := \frac{1}{12} \cdot t_{f.c} \cdot b_{f.c}^{\ 3} = 666.7\ in^4$

Effective moment of inertia: $I_{y.eff} := I_{y.c} + \left(\frac{t}{c}\right) \cdot I_{y.t} = \left(2.1 \cdot 10^3\right)\ in^4$

Therefore, the required torsional stiffness of the cross-frame is given as:

$$\beta_{T.req} := \frac{3.6\ L}{\phi_{br} \cdot n_b \cdot E \cdot I_{y.eff}} \cdot \left(\frac{\gamma_{CL} \cdot M_r}{C_b}\right)^2 = \left(6.78 \cdot 10^4\right)\ \frac{kip \cdot in}{rad}$$

Now that the required stiffness has been established, the next step is to estimate the actual stiffness of cross-frame and verify its adequacy. As outlined extensively in Yura (2001) and the proposed Article 6.7.4.2.2, the torsional stiffness of a cross-frame must consider the effects of not only the brace itself, but also the effects of web distortion, in-plane girder, and its connections. The calculations herein evaluate each component of stiffness and then consider the combined effects against the required stiffness.

First, the stiffness of the brace is evaluated. The torsional stiffness of a X-type cross-frame can be estimated as the following expression, assuming a compression system (Yura, 2001):

$$\beta_b := R_{con} \cdot \left(\frac{A_d \cdot E \cdot s_g^{\ 2}\ h_b^{\ 2}}{L_d^{\ 3}}\right)$$

To solve for the torsional brace stiffness, several variables related to the cross-frame proportions must be established. Many of these variables have been previously defined but are presented again for reference.

Another important aspect is the inherent flexibility with the eccentric end connections of the cross-frame members. The connection stiffness is typically considered by assigning a modification factor to the stiffness of the brace. As highlighted previously, AASHTO *LRFD* recommended using a modification factor (R-factor) of 0.65 when evaluating cross-frames for stability-related applications. As such, that value is used here.

Modulus of elasticity, steel: $E = 29000\ ksi$

Girder spacing: $s_g = 132\ in$

Height of cross-frame brace: $h_b = 72\ in$

Diagonal area: $A_d := A_g = 11.4\ in^2$

Strut area: $A_s := A_g = 11.4\ in^2$

Length of diagonal: $L_d = 150.4\ in$

Stability modification factor (construction): $R_{con} := 0.65$

Therefore, the torsional stiffness of the K-type cross-frame is given by the following, when considering the inherent flexibility of the connections:

$$\beta_b := R_{con} \cdot \left(\frac{A_d \cdot E \cdot {s_g}^2 \ {h_b}^2}{{L_d}^3} \right) = \left(5.71 \cdot 10^6\right) \frac{kip \cdot in}{rad}$$

Note that the actual stiffness of the cross-frame is considerably larger than the required stiffness for the system; however, the brace stiffness is only one component of the total stiffness. As such, other components (i.e., cross-sectional distortion and in-plane girder effects) are considered herein. The total stiffness is then solved using the expression for springs in series.

With that in mind, the web-distortional effects are considered based on the expression developed by Yura (2001). Note that web-distortional effects are generally only critical when a shallow brace is used relative to the girder depth and partial-depth stiffeners are used; this is most common when diaphragm beams are used as braces rather than cross-frames. Cross-frames, like the ones used in this design example, typically brace the full depth of the girder web. In the proposed AASHTO *LRFD* provisions, the stiffness component related to distortion can be neglected when the diaphragm or cross-frame is at least 80% of the girder depth. In this scenario, a 3-inch gap is assumed between the edge of the gusset plates and the inside face of top and bottom flanges such, web distortional effects are expected to be negligible. For the sake of completeness, a full calculation is presented below.

The following parameters characterize the dimensions of the cross-frames and connection plate stiffeners. A separate stiffness is evaluated for the top clear distance and the bottom clear distance. Ultimately, the web distortion stiffness is the combined effect of both contributions.

Flange centroidal distance: $h_o := 85\ in$

Clear distance outside brace: $h_i := 3\ in$

Stiffener thickness: $t_s := 0.5\ in$

Stiffener width: $b_s := 12\ in$

Web thickness: $t_w = 0.563\ in$

Therefore, the web distortional stiffness is computed as follows. Note that the value is orders of magnitude higher than the brace stiffness, as expected.

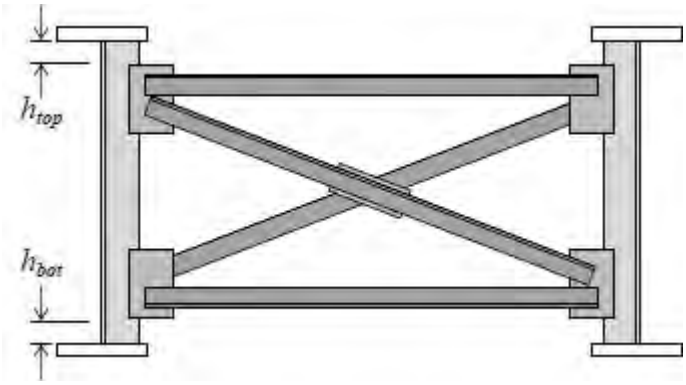

Figure 9: Schematic showing the definition of important cross-sectional distortion variables

$$\beta_{top} := \frac{3.3\ E}{h_i} \cdot \left(\frac{h_o}{h_i}\right)^2 \cdot \left(\frac{1.5\ h_i \cdot {t_w}^3}{12} + \frac{t_s \cdot {b_s}^3}{12}\right) = \left(1.8 \cdot 10^9\right)\ \frac{kip \cdot in}{rad}$$

$$\beta_{bot} := \beta_{top} = \left(1.8 \cdot 10^9\right)\ \frac{kip \cdot in}{rad}$$

$$\beta_{sec} := \frac{1}{\left(\frac{1}{\beta_{top}} + \frac{1}{\beta_{bot}}\right)} = \left(9.2 \cdot 10^8\right)\ \frac{kip \cdot in}{rad}$$

Lastly, the in-plane girder stiffness is computed. The in-plane girder stiffness is generally only critical for narrow superstructures such as those with two or three girders across the width. For redundant systems with significant bridge width, the in-plane stiffness is general much larger than the brace stiffness. The following parameters describe the general layout of the framing plan. Note that the moment of inertia was previously computed in the original SBDH example (section G4-1).

Number of girders: $n_g := 4$

Moment of inertia about x-axis: $I_x := 118984\ in^4$

Span length: $L = 160\ ft$

Therefore, the in-plane girder stiffness is computed as follows. Note that the value is similar to that of the brace stiffness, given that the span is relatively narrow, but not enough to warrant serious consideration of system buckling (Yura, 2008; Han and Helwig, 2020).

$$N_g := \frac{24\ \left(n_g - 1\right)^2}{n_g} = 54$$

$$\beta_g := \frac{N_g\ {s_g}^2\ E \cdot I_x}{L^3} = 458696\ \frac{kip \cdot in}{rad}$$

The total, combined effect of each component is considered through a "spring in series" analogy. Note that the total stiffness is always less than the smallest of the three individual stiffness components. Given that full depth web stiffeners and a deep cross-frame was used in this example, the inverse of the cross-sectional distortion term is extremely small. Had this term been neglected altogether, as permitted in the proposed AASHTO *LRFD* Article 6.7.4.2.2, the system stiffness would be nearly identical to what is shown below.

$$\beta_T := \frac{1}{\left(\frac{1}{\beta_b} + \frac{1}{\beta_{sec}} + \frac{1}{\beta_g}\right)} = \left(4.24 \cdot 10^5\right)\ \frac{kip \cdot in}{rad}$$

Finally, the total brace stiffness is evaluated against the required stiffness as shown in the calculations below:

Total stiffness: $\beta_T = \left(4.2 \cdot 10^5\right)\ \frac{kip \cdot in}{rad}$

Required stiffness: $\beta_{T.req} = \left(6.8 \cdot 10^4\right)\ \frac{kip \cdot in}{rad}$

$$Check := \left\| \begin{array}{l} \text{if } \beta_T \geq \beta_{T.req} \\ \quad \| \text{“OK”} \\ \text{else} \\ \quad \| \text{“N.G.; Refine Design”} \end{array} \right\| = \text{“OK”}$$

Therefore, the cross-frame panel comprised of L8x8x3/4 single-angle sections is adequate in terms of stability bracing stiffness by a large margin. However, recall from the strength and fatigue limit state calculations that a smaller section is warranted given the reserve capacity. If the designer chooses to re-evaluate the design with a smaller angle section, then the bracing stiffness check would also need to be re-examined.

References

American Association of State Highway and Transportation Officials. 2014. *G13.1 Guidelines for Steel Girder Bridge Analysis.* 2nd Ed.

American Association of State Highway and Transportation Officials. 2020. *LRFD Bridge Design Specifications.* 9th Ed. Washington, D.C.

American Institute of Steel Construction. 2010. *Specification for Structural Steel Buildings.* 14th Ed. Chicago, IL.

American Institute of Steel Construction. 2016. *Specification for Structural Steel Buildings.* 15th Ed. Chicago, IL.

Barth, K. 2015. *Steel Bridge Design Handbook Design Example 2A: Two-Span Continuous Straight Composite Steel I-Girder Bridge.* Washington, DC: Federal Highway Administration.

Battistini, A., W. Wang, T. Helwig, M. Engelhardt, and K. Frank. 2016. "Stiffness Behavior of Cross Frame in Steel Bridge Systems." *Journal of Bridge Engineering* (American Society of Civil Engineers) 21 (6).

Han, L., and T. Helwig. 2020. Elastic Global Lateral Buckling of Straight I-Shaped Girder Systems.” *Journal of Structural Engineering* (American Society of Civil Engineers) 146 (4).

Helwig, T., and J. Yura. 2015. *Steel Bridge Design Handbook: Bracing System Design*. Washington, DC: Federal Highway Administration.

Liu, Y., and T. Helwig. 2020a. "Torsional Brace Strength Requirements for Steel I-Girder Systems." *Journal of Bridge Engineering* (American Society of Civil Engineers) 146 (1).

Liu, Y., B. Kovesdi, and T. Helwig. 2020b. "Torsional Bracing Stiffness Requirements for Steel I-Girder Systems." *Journal of Structural Engineering* (American Society of Civil Engineers). [Under Revision]

Rivera, J., and B. Chavel. 2015. *Steel Bridge Design Handbook Design Example 3: Three-Span Continuous Horizontally Curved Composite Steel I-Girder Bridge.* Washington, DC: Federal Highway Administration.

Stith, J., A. Schue, J. Farris, B. Petruzzi, T. Helwig, E. Williamson, K. Frank, M. Engelhardt, and J. Kim. 2010. *Guidance for Erection and Construction of Curved I-Girder Bridges*. TxDOT Report 0-5574-1: Center for Transportation Research, The University of Texas at Austin.

White, D., D. Coletti, B. Chavel, A. Sanchez, C. Ozgur, J. Jimenez Chong, R. Leon, et al. 2012. *Guidelines for Analysis Methods and Construction Engineering of Curved and Skewed Steel Girder Bridges.* NCHRP Report 725, Washington, D.C.: Transportation Research Board.

White, D., T. Nguyen, D. Coletti, B. Chavel, M. Grubb, and C. Boring. 2015. *Guidelines for Reliable Fit-Up of*

Steel I-Girder Bridges. NCHRP 20-07/Task 355, Washington, D.C.: Transportation Research Board, National Research Council.

Yura, J. 2001. "Fundamentals of Beam Bracing." *Engineering Journal* (American Institute of Steel Construction) 11-26.

Yura, J., T. Helwig, R. Herman, and C. Zhou. 2008. "Global Lateral Buckling of I-Shaped Girder Systems." *Journal of Structural Engineering* (American Institute of Steel Construction) 134 (9).